Oxygen-derived free radical and active oxygen complex formation from cobalt(II) chelates in vitro

ARTICLE *in* CHEMICAL RESEARCH IN TOXICOLOGY · JANUARY 1992

Impact Factor: 3.53 · DOI: 10.1021/tx00025a019 · Source: PubMed

3 AUTHORS, INCLUDING:

Maria Kadiiska
National Institute of Environmental Health S…
120 PUBLICATIONS **4,182** CITATIONS
SEE PROFILE

Ronald P Mason
National Institute of Environmental Health S…
565 PUBLICATIONS **21,036** CITATIONS
SEE PROFILE

(13) Sterzel, W., Bedford, P., and Eisenbrand, G. (1985) Automated determination of DNA using fluorochrome Hoechst 33258. *Anal. Biochem.* 147, 462–467.
(14) Meyn, R. E., Grdnina, D. J., and Fletcher, S. E. (1980) Repair of radiation damage *in vivo*. In *Radiation Biology in Cancer Research* (Meyn, R. E., and Withers, R., Eds.) pp 95–102, Raven Press, New York.
(15) Heidmann, M., Fonrobert, P., Przybylski, M., Platt, K. L., Seidel, A., and Oesch, F. (1988) Conjugation reactions of polyaromatic quinones to mono- and bis-glutathionyl adducts: direct analysis by fast atom bombardment mass spectrometry. *Biomed. Environ. Mass Spectrom.* 14, 329–334.
(16) Wirth, K. P., Junker, E., Roellgen, F. W., Fonrobert, P., and Przybylski, M. (1989) Effects of cosolvents in glycerol assisted dynamic SIMS. *Adv. Mass Spectrom.* 11A, 430–431.
(17) Stahl, W., Krauth-Siegel, R. L., Schirmer, R. H., and Eisenbrand, G. (1987) A method to determine the carbamoylating potential of 1-(2-chloroethyl)-1-nitrosoureas. *IARC Sci. Publ.* 84, 191–193.
(18) Eisenbrand, G., and Habs, M. (1980) Chronic toxicity and carcinogenicity of cytostatic N-Nitroso-(2-chloroethyl)ureas after repeated intravenous application to rats. In *Mechanisms of Toxicity and Hazard Evaluation* (Holmstedt et al., Eds.) pp 273–278, Elsevier, Amsterdam.
(19) Weiss, R. B., Poster, D. S., and Penta, J. S. (1981) The nitrosoureas and pulmonary toxicity. *Cancer Treat. Rev.* 8, 111–124.

Oxygen-Derived Free Radical and Active Oxygen Complex Formation from Cobalt(II) Chelates in Vitro

Phillip M. Hanna,* Maria B. Kadiiska,† and Ronald P. Mason

National Institute of Environmental Health Sciences, National Institutes of Health, P.O. Box 12233, Research Triangle Park, North Carolina 27709

Received July 8, 1991

The electron paramagnetic resonance (EPR) spin trapping technique was used to study the generation of oxygen free radicals from the reaction of hydrogen peroxide with various Co(II) complexes in pH 7.4 phosphate buffer. The 5,5-dimethyl-1-pyrroline *N*-oxide (DMPO) spin trap was used in these experiments to detect superoxide and hydroxyl free radicals. Superoxide radical was generated from the reaction of H_2O_2 with Co(II), but was inhibited when Co(II) was chelated with adenosine 5′-diphosphate or citrate. Visible absorbance spectra revealed no change in the final oxidation state of the cobalt ion in these samples. The EDTA complex also prevented detectable free-radical formation when H_2O_2 was added, but visible absorbance data indicated oxidation of the Co(II) to Co(III) in this case. The amount of DMPO/•OOH adduct detected by EPR was greatly enhanced when H_2O_2 reacted with the nitrilotriacetate complex relative to Co(II) alone, and in addition, concurrent formation of the DMPO/•OH adduct due to slow oxidation of Co(II) was observed. The hydroxyl radical adduct formation was suppressed by ethanol, but not DMSO, indicating that free hydroxyl radical was not formed. The deferoxamine nitroxide radical was exclusively formed when H_2O_2 was added to the Co(II) complex of this ligand, most probably in a site-specific manner. In the presence of ethylenediamine, Co(II) bound molecular O_2 and directly oxidized DMPO to its DMPO/•OH adduct without first forming free superoxide, hydroxyl radical, or hydrogen peroxide. An experiment using ^{17}O-enriched water revealed that the Co(II)–ethylenediamine complex caused the DMPO to react with solvent water to form the DMPO/•OH adduct. The relevance of these results to toxicological studies of cobalt is discussed.

Introduction

Cobalt is an essential element in the human diet but, as with most metals, it is toxic in higher doses (*1*). The deleterious effects of cobalt toxicity are varied, and large doses of cobalt salts are believed to be carcinogenic (*1–3*), cause DNA damage (*4–6*), suppress hepatic hemoproteins, especially cytochrome P-450 (*7–10*), and contribute to chronic blood disorders (*11, 12*), among other effects (*12*).

The chemical mechanisms through which cobalt salts exert their toxicity in vivo may involve, at least in part, the formation of active oxygen species such as the highly reactive hydroxyl radical. Under physiological conditions in vitro, Co(II) has been reported to promote the formation of hydroxyl radicals or "reactive species" from hydrogen peroxide, which then proceeded to degrade deoxyribose sugar and hydroxylate aromatic compounds (*13, 14*). Promotion of both lipid peroxidation (*14, 15*) and site-specific hydroxyl radical damage to DNA (*4, 5*) by Co(II) and hydrogen peroxide in vitro have also been reported. However, direct EPR[1] experiments using the spin trapping technique have shown clearly that the superoxide anion, not free hydroxyl radical, is generated by Co(II) when hydrogen peroxide is added in pH 7.4 phosphate buffer (*16*). The mechanism through which superoxide is generated from Co(II) and H_2O_2 has yet to be determined, but

† Permanent address: Institute of Physiology, Bulgarian Academy of Sciences, 1113 Sofia, "Academician Georgy Bonchev" Street, Building 23, Bulgaria.

[1] Abbreviations: EPR, electron paramagnetic resonance; SOD, superoxide dismutase; NTA, nitrilotriacetic acid; ADP, adenosine 5′-diphosphate; EDTA, ethylenediaminetetraacetic acid; DFO, deferoxamine mesylate; DMPO, 5,5-dimethyl-1-pyrroline *N*-oxide; DMSO, dimethyl sulfoxide.

does not seem to involve the reduction of O_2 (*16*).

Clearly, the formation of active oxygen species in solutions containing Co(II) and its relevancy to biology are not fully understood. In this report, the effects of various ligands on the reaction of Co(II) with hydrogen peroxide under physiological conditions were investigated using EPR and visible absorption spectroscopies. The results demonstrate that the formation of active oxygen species from Co(II) and hydrogen peroxide is highly influenced by the kind of cobalt chelate present. The type of active oxygen species generated by each complex also varies greatly. The relevance of these results with respect to previous reports in the literature is discussed. Furthermore, our results provide definitive proof for the direct oxidation of the 5,5-dimethyl-1-pyrroline *N*-oxide spin trap to its 2-hydroxy nitroxyl radical adduct by a Co(II)–ethylenediamine complex and dioxygen without first generating hydroxyl radicals. This latter result is presented as a caveat with respect to working with spin traps in the presence of metal ions.

Materials and Methods

SOD from bovine erythrocytes (EC 1.15.1.1; specific activity = 5000 units/mg) and catalase from bovine liver (EC 1.11.1.6; specific activity = 65 000 units/mg) were purchased from Boehringer Mannheim Biochemicals (Indianapolis, IN). Cobalt(II) sulfate (99.999%), citric acid (trisodium salt, 99%), NTA (disodium salt, 99+%), and ethylenediamine (99+%) were obtained from Aldrich (Milwaukee, WI); ADP (potassium salt, grade XIX, from equine muscle), EDTA (disodium salt), DFO, and DMPO were from Sigma (St. Louis, MO); DMSO and 30% hydrogen peroxide were from Fisher (Fair Lawn, NJ); monosodium phosphate and disodium phosphate were from Mallinckrodt (Paris, KY); and Chelex 100 chelating resin was from Bio-Rad (Richmond, CA). ^{17}O-Enriched water was purchased from MSD Isotopes (Montreal, Canada) in sealed glass ampules.

Buffer solutions (pH 7.4) were dialyzed against preequilibrated Chelex 100 resin to remove trace transition metal ions. Metal-free glassware (soaked in 50% sulfuric acid and rinsed thoroughly with deionized water) was used to prepare all solutions which, except for the Chelex-treated buffer solutions, were prepared daily. DMPO obtained from Sigma was purified by vacuum sublimation and stored at −70 °C under a nitrogen atmosphere.

Unless indicated otherwise, samples were 2.5 mM in Co(II) and 5.0 mM in H_2O_2. Whenever used, SOD and catalase concentrations were 25 and 50 μg/mL, respectively, unless indicated otherwise. For samples containing cobalt complexes, the appropriate ligand solution was added to a cobalt solution before any other solution was added, and the hydrogen peroxide was added last. For samples with ethylenediamine, however, the cobalt solution was added last since O_2 binding by the cobalt–ethylenediamine complex becomes important (see Results). All samples contained 100 mM DMPO, which was thawed and used the same day to avoid excessive degradation at room temperature.

EPR spectra were recorded at room temperature using a Varian E-109 spectrometer operating at 9.33 GHz with a 100-kHz modulation frequency. A microwave power of 20 mW and modulation amplitude of 0.33 G were typically employed. Spectra were simultaneously recorded on an IBM-compatible computer interfaced to the spectrometer.[2] The samples were Vortex-mixed and then aspirated to a quartz aqueous cell (Wilmad) prepositioned in a TM_{110} microwave cavity. EPR data collection was initiated exactly 1 min after the addition of hydrogen peroxide (or cobalt in the case of the ethylenediamine complex). Computer simulations of the experimental data were obtained using a program[2] which sequentially varied each parameter until a true minimum in the error surface was located.

Visible absorption spectra were recorded on a Hewlett Packard 8451A diode array spectrophotometer, and O_2 consumption experiments were monitored with a Clark oxygen electrode (Yellow Springs Instrument Co.).

[2] EPR computer programs were written in these labs by Mr. David R. Duling.

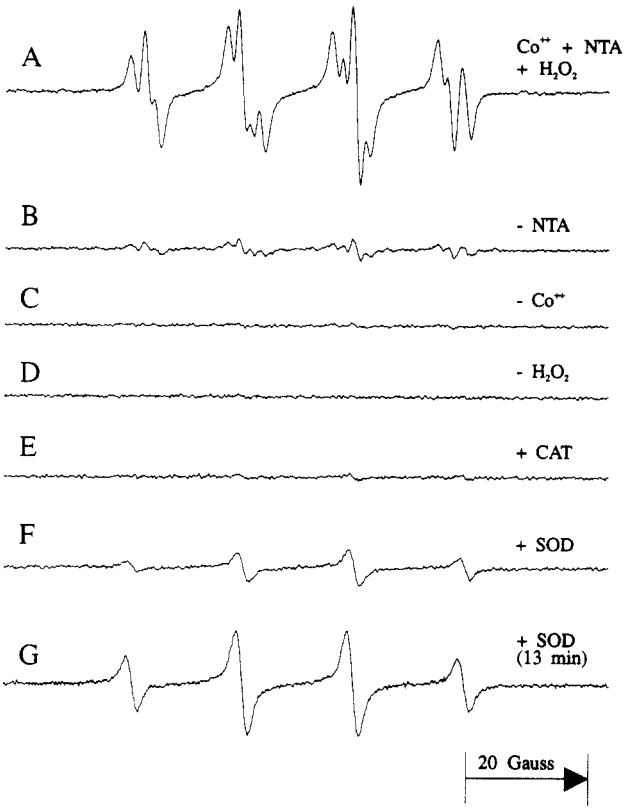

Figure 1. (A) EPR spectrum obtained from 2.5 mM Co(II), 2.75 mM nitrilotriacetate (NTA), 5 mM H_2O_2, and 100 mM DMPO in pH 7.4 phosphate buffer. The reaction was initiated by the addition of H_2O_2 and the scan initiated 1 min after mixing. Instrumental conditions: 20 mW microwave power, 0.33 G modulation amplitude, 1.0×10^4 gain, 0.128 s time constant, 40 G/min sweep rate. (B) As in (A), but without NTA. (C) As in (A), but without Co(II). (D) As in (A), but without H_2O_2. (E) As in (A), but with 50 μg/mL catalase (CAT). (F) As in (A), but with 25 μg/mL superoxide dismutase (SOD). (G) As in (F), but this is a second scan initiated 13 min after mixing.

Results

Oxygen Radicals from Co(II) Complexes with Hydrogen Peroxide. The generation of oxygen radicals from the reaction of Co(II) with hydrogen peroxide in the presence of various biologically important ligands was investigated. Except for the experiments with deferoxamine (DFO), the spin trap used was 5,5-dimethyl-1-pyrroline *N*-oxide (DMPO).

(a) Nitrilotriacetate Ligand. As previously reported (*16*), Co(II) and H_2O_2 in pH 7.4 phosphate buffer generated the superoxide radical (Figure 1B). The amount of superoxide trapped by DMPO (DMPO/•OOH; a^N = 14.2 G, a^H_β = 11.2 G, and a^H_γ = 1.2 G) increased 10–12 times in the presence of NTA (Figure 1A). Enhanced superoxide production was also supported by O_2-evolution experiments using a Clark oxygen electrode (data not shown). Increasing the Co:NTA ratio to 1:2.2 only slightly increased the DMPO/•OOH EPR signal intensity. The role of both Co(II) and H_2O_2 in the formation of the DMPO/•OOH adduct is demonstrated in Figure 1C–E, and 25 μg/mL SOD inhibited its formation completely (Figure 1F), indicating that the superoxide was free in solution. In the presence of SOD, however, a four-line EPR signal from an apparent hydroxyl radical adduct with DMPO (DMPO/•OH; a^N = 14.9 G and a^H_β = 14.9 G) was observed, which

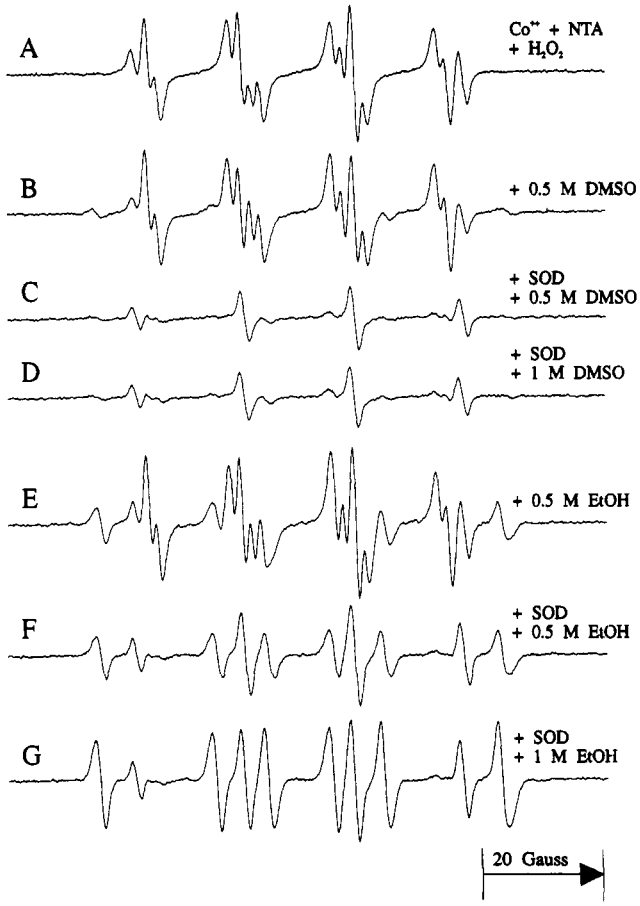

Figure 2. (A) EPR spectrum obtained from 2.5 mM Co(II), 2.75 mM nitrilotriacetate (NTA), 5 mM H_2O_2, and 100 mM DMPO in pH 7.4 phosphate buffer. The reaction was initiated by the addition of H_2O_2 and the scan initiated 1 min after mixing. Instrumental conditions were the same as in Figure 1. (B) As in (A), but with 0.5 M DMSO. (C) As in (B), but with 25 μg/mL superoxide dismutase (SOD). (D) As in (C), but with 1 M DMSO. (E) As in (A), but with 0.5 M ethanol (EtOH). (F) As in (E), but with 25 μg/mL SOD. (G) As in (F), but with 1 M EtOH.

slowly increased with time (Figure 1F,G).

The four-line DMPO/•OH signal was not diminished in the presence of up to 1 M DMSO (Figure 2B–D). DMSO is a free hydroxyl radical scavenger and generates a six-line signal due to subsequent formation of the DMPO/•CH_3 adduct, which was only barely noticeable here (Figure 2B). Thus, it is apparent that free hydroxyl radical was not generated from the reaction of the NTA complex with hydrogen peroxide.

A six-line EPR signal from DMPO/•$CH(OH)CH_3$ with a^N = 15.8 G and a^H_β = 22.9 G was observed, however, when the reaction was carried out in the presence of ethanol, another commonly used free hydroxyl radical scavenger (Figure 2E–G). As with 1 M DMSO, the DMPO/•OH adduct was not diminished by 1 M ethanol. The slower production of this oxidant relative to that of superoxide radical from the NTA complex may be attributed to the slow oxidation of Co(II) to Co(III) by H_2O_2. This is illustrated in Figure 3A where the Co(III) absorbance maxima of the NTA complex appear at 393 and 562 nm. These compare well with maxima previously reported for the 1:1 NTA complex of Co(III) in aqueous (pH 5.9) medium at 395 nm (ϵ_{max} = 111 M^{-1} cm^{-1}) and 560 nm (ϵ_{max} = 117 M^{-1} cm^{-1}) (*17*). Using the reported molar absorptivity at 395 nm, only about 20% of the cobalt was oxidized to Co(III) within 15 min of H_2O_2 addition. Alternatively, the Co(III)–NTA complex may dimerize to yield a bridged complex with two μ-hydroxo ligands and absorption

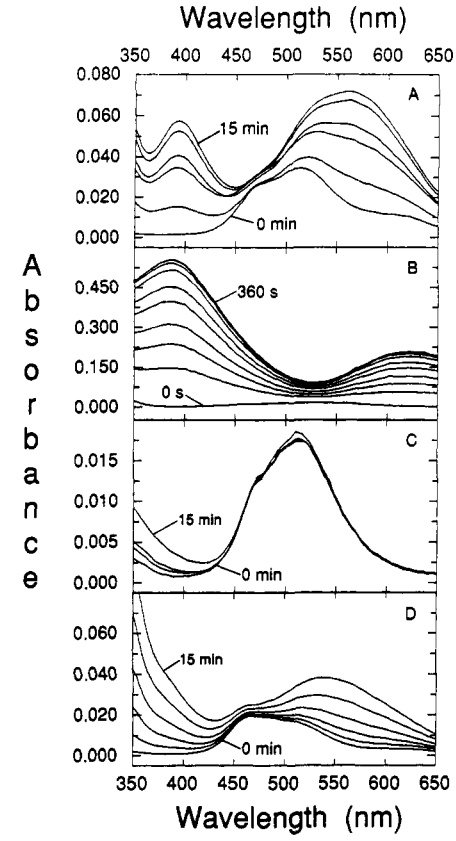

Figure 3. (A) Visible absorbance spectra obtained from 2.5 mM Co(II), 2.75 mM nitrilotriacetate (NTA), and 5 mM H_2O_2 in pH 7.4 phosphate buffer. The reaction was initiated by the addition of H_2O_2, and the 1-s scans were taken at 0, 1, 3, 5, 10, and 15 min after mixing. (B) Visible absorbance spectra obtained from 2.5 mM Co(II), 2.75 mM deferoxamine (DFO), and 5 mM H_2O_2 in pH 7.4 phosphate buffer. The reaction was initiated by the addition of H_2O_2, and the 1-s scans were taken at 0, 20, 40, 60, 90, 120, 180, 240, 300, and 360 s after mixing. (C) Visible absorbance spectra obtained from 2.5 mM Co(II), 8.25 mM adenosine 5′-diphosphate (ADP), and 5 mM H_2O_2 in pH 7.4 phosphate buffer. The reaction was initiated by the addition of H_2O_2, and the 1-s scans were taken at 0, 1, 3, and 15 min after mixing. (D) Visible absorbance spectra obtained from 2.5 mM Co(II), 2.75 mM ethylenediaminetetraacetate (EDTA), and 5 mM H_2O_2 in pH 7.4 phosphate buffer. The reaction was initiated by the addition of H_2O_2, and the 1-s scans were taken at 0, 1, 3, 6, 10, and 15 min after mixing.

maxima at 397 nm (ϵ_{max} = 395 M^{-1} cm^{-1}) and 568 nm (ϵ_{max} = 296 M^{-1} cm^{-1}) (*17*). In this case, only about 12% of the cobalt would have been in the Co(III) oxidation state after 15 min. At pH 7.4, the dimer complex would ultimately dominate (*17*), though the $[Co(NTA)(OH)(OH_2)]^-$ complex may form initially.

(b) Deferoxamine Ligand. When Co(II) was complexed with deferoxamine, oxidation by H_2O_2 to Co(III) was complete within 5 min, as shown in Figure 3B. The resulting oxidant produced from the Fenton-like reaction was efficiently trapped by the deferoxamine ligand to form the distinctive deferoxamine nitroxide radical signal with a^N = 7.7 G and a^H = 6.2 G (2 H) [Figure 4A (*18*, *19*)], such that neither the DMPO/•OH nor the DMPO/•OOH adduct was detected when 100 mM DMPO was present. A residual nitroxide signal was observed when deferoxamine alone was mixed with hydrogen peroxide (Figure 4B), possibly due to trace metal contaminants in the deferoxamine solution itself. No signal was detected, however, when either deferoxamine or hydrogen peroxide was omitted (Figure 4C,D), or when catalase was added to the complete system (Figure 4E). As expected for a Fenton-

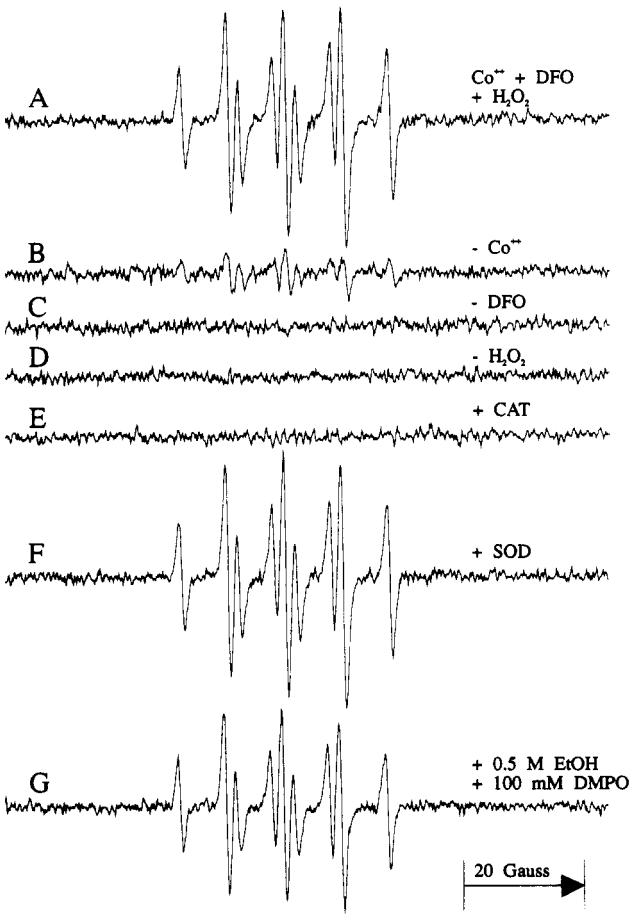

Figure 4. (A) EPR spectrum obtained from 2.5 mM Co(II), 2.75 mM deferoxamine mesylate (DFO), 5 mM H_2O_2, and 100 mM DMPO in pH 7.4 phosphate buffer. The reaction was initiated by the addition of H_2O_2 and the scan initiated 1 min after mixing. Instrumental conditions: 4.0×10^4 gain, 0.25 s time constant, and 20 G/min sweep rate; all other settings are the same as in Figure 1. (B) As in (A), but without Co(II). (C) As in (A), but without DFO. (D) As in (A), but without H_2O_2. (E) As in (A), but with 50 μg/mL catalase (CAT). (F) As in (A), but with 25 μg/mL superoxide dismutase (SOD). (G) As in (A), but with 0.5 M ethanol (EtOH) and 100 mM DMPO.

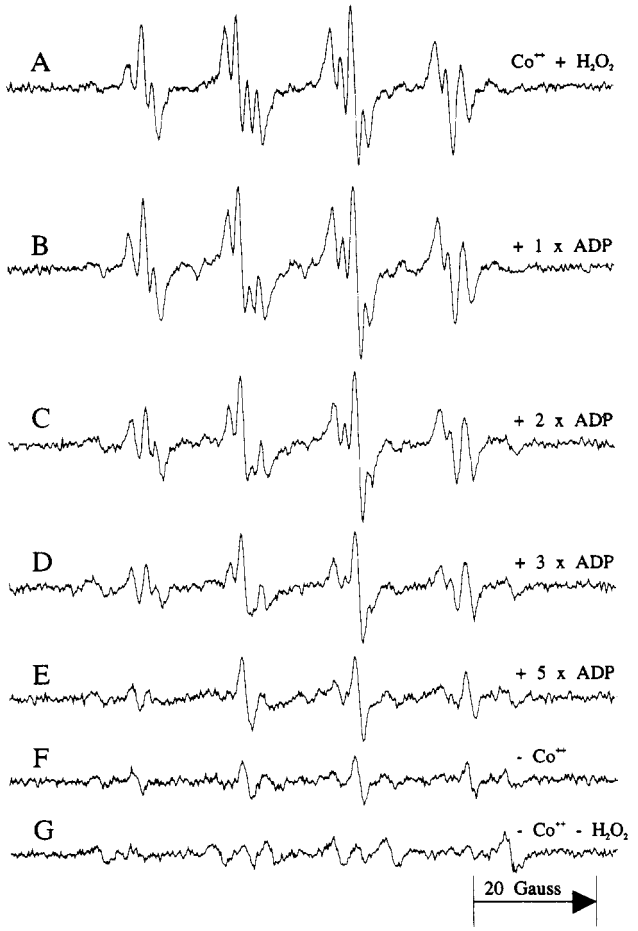

Figure 5. (A) EPR spectrum obtained from 2.5 mM Co(II), 5 mM H_2O_2, and 100 mM DMPO in pH 7.4 phosphate buffer. The reaction was initiated by the addition of H_2O_2 and the scan initiated 1 min after mixing. Instrumental conditions: 5.0×10^4 gain; all other settings were the same as in Figure 4. (B) As in (A), but with 2.75 mM adenosine 5′-diphosphate (ADP). (C) As in (A), but with 5.5 mM ADP. (D) As in (A), but with 8.25 mM ADP. (E) As in (A), but with 13.75 mM ADP. (F) As in (D), but without Co(II). (G) As in (D), but without Co(II) and H_2O_2.

like reaction, SOD had no effect on the formation of the nitroxide adduct (Figure 4F).

The presence of 0.5 M ethanol in the Co(II)–DFO mixture did not significantly diminish the deferoxamine nitroxide radical formation upon H_2O_2 addition. The experiment was repeated with 100 mM DMPO present, and as expected, no signal from the DMPO/$^{\bullet}$CH(OH)CH_3 adduct (formed when ethanol scavenges free hydroxyl radical) was detected (Figure 4G).

(c) ADP, Citrate, and EDTA Ligands. Figure 5 illustrates the inhibitory effect of ADP on the generation of the superoxide radical adduct from Co(II) and H_2O_2. The Co(II)–ADP complex does not show any significant change in the Co(II) absorbance maximum at 512 nm within 15 min (Figure 3C). The residual four-line DMPO/$^{\bullet}$OH signal observed in Figure 5, spectra F and G, was due to this impurity in the DMPO.

The effect of citrate on the Co(II) and H_2O_2 reaction was very similar to that of ADP (data not shown). The generation of superoxide from hydrogen peroxide and Co(II) was restricted in the presence of citrate (Co:citrate = 1:3.3) in the same manner as with ADP. In addition, no significant change in the visible spectrum was detected up to 15 min after hydrogen peroxide was mixed with Co(II) and citrate.

On the other hand, and in agreement with previously reported results (*16*), a Co:EDTA ratio of 1:1.1 was sufficient to completely inhibit the detection of superoxide from H_2O_2 and Co(II) in phosphate (data not shown). In this complex with EDTA, as with NTA, Co(II) was slowly oxidized to Co(III), shown by a slow increase in the visible absorbance at 536 nm in Figure 3D. However, no free hydroxyl radical was trapped by DMPO in the EPR experiment (data not shown). It is possible that the EDTA ligand was itself oxidized in a site-specific manner, similar to the reaction of H_2O_2 with the Co(II)–DFO complex, but the oxidized ligand was not observable by EPR under the experimental conditions used.

(d) Ethylenediamine Ligand. In the presence of a 3.3-fold excess of ethylenediamine (en) relative to the Co(II), an EPR signal from the DMPO/$^{\bullet}$OH adduct was observed (a^N = 14.9 G and a_β^H = 14.9 G) regardless of whether or not H_2O_2 was added to the sample (Figure 6A). For these samples Co(II) was added last to initiate the reaction, though similar results were obtained when H_2O_2 was added last. In either case, no DMPO/$^{\bullet}$OOH adduct was detected. The signal from the DMPO/$^{\bullet}$OH adduct continued to gain intensity 4 min after Co(II) was mixed with ethylenediamine in pH 7.4 phosphate buffer (Figure 6B), indicating a relatively slow reaction rate. Both Co(II) and ethylenediamine were necessary for the reaction to occur (Figure 6C,D), and similar results were obtained

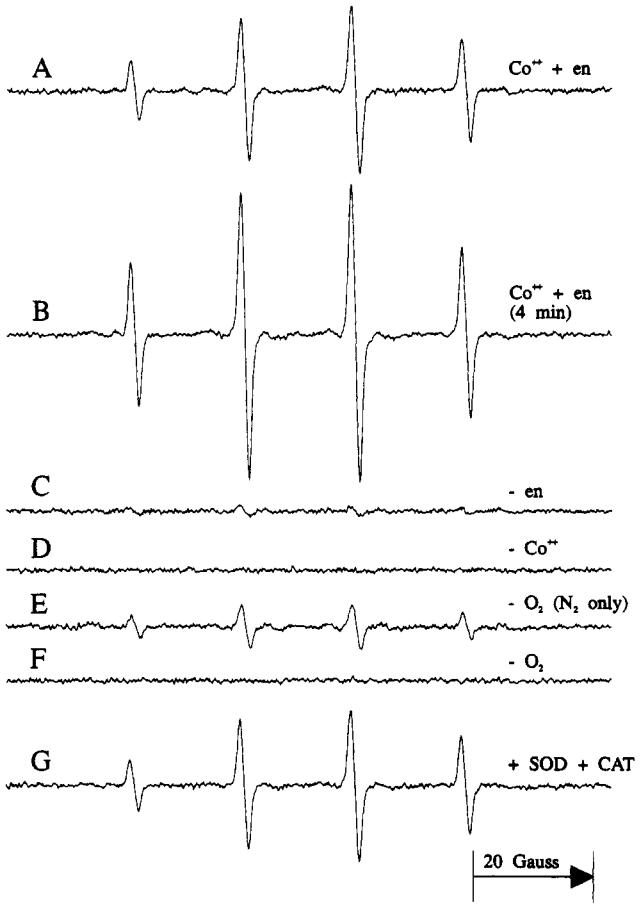

Figure 6. (A) EPR spectrum obtained from 2.5 mM Co(II), 8.25 mM ethylenediamine (en), and 100 mM DMPO. The reaction was initiated by the addition of Co(II), and the scan was initiated 1 min after mixing. Instrument settings were the same as in Figure 1. (B) As in (A), but this is a second scan initiated 4 min after mixing. (C) As in (A), but without ethylenediamine. (D) As in (A), but without Co(II). (E) As in (A), but the solution was first bubbled with N_2 before Co(II) addition. (F) As in (E), but with 25 units/mL glucose oxidase, 5 mM β-D-glucose, and 50 μg/mL catalase to remove trace O_2. (G) As in (A), but with 50 μg/mL superoxide dismutase (SOD) and 50 μg/mL catalase (CAT).

when the Co:en ratio was only 1:2.2 (data not shown).

Since amino and polyamino complexes of Co(II) are known to bind O_2 (*20*), the reaction was carried out under anaerobic conditions. When a solution of DMPO and ethylenediamine was first bubbled with N_2 gas before Co(II) was added, the resultant DMPO/•OH EPR signal was significantly decreased (Figure 6E). This experiment was repeated in the presence of glucose oxidase and glucose to consume the residual O_2 after first bubbling with N_2 (plus catalase to consume the H_2O_2 formed as a consequence), and absolutely no signal was detected (Figure 6F). A signal was observed, however, after admittance of air to this latter sample, and the presence of glucose alone did not affect the formation of the DMPO/•OH adduct (data not shown).

The role of molecular oxygen in the formation of the DMPO/•OH adduct was further supported by the O_2 consumption experiment shown in Figure 7. Within the first minute after addition of Co(II) to ethylenediamine in pH 7.4 phosphate, more than 85% of the available dioxygen in solution was taken up by the cobalt complex, which increased to more than 95% after 3 min. In comparison, Co(II) alone or a Co(II) complex with NTA (Co:NTA = 1:1.1) did not take up dioxygen in solution (Figure 7). Furthermore, the appearance of a large absorbance shoulder at approximately 380 nm in the visible

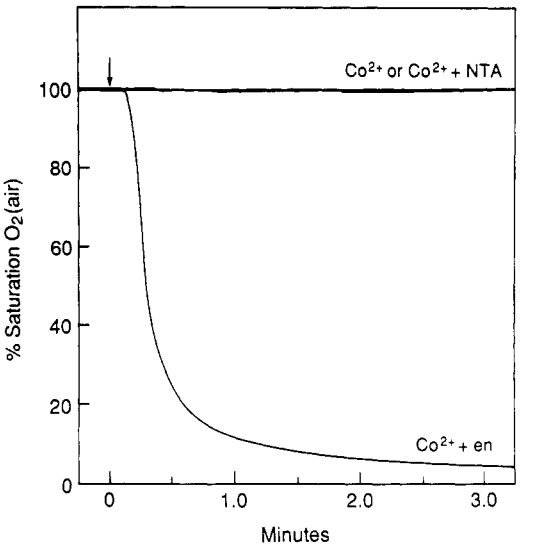

Figure 7. Oxygen consumption time profile in pH 7.4 phosphate buffer following the addition of 2.5 mM Co(II) to 8.25 mM ethylenediamine (en) or 2.75 nitrilotriacetate (NTA). In the control, 2.5 mM Co(II) was added to phosphate buffer alone. The traces for Co(II) with NTA and the control were identical.

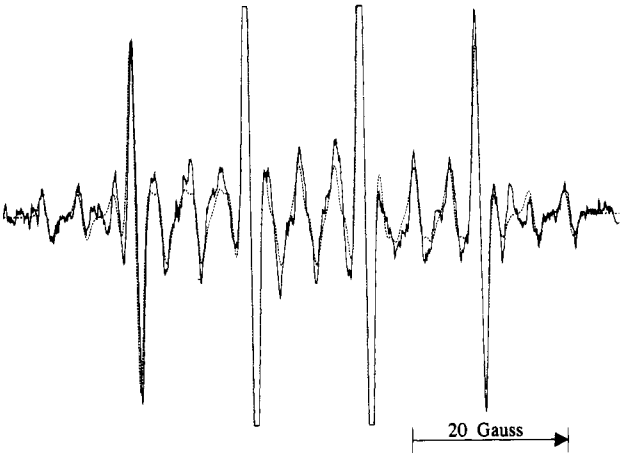

Figure 8. EPR spectrum obtained from 2.5 mM Co(II) and 8.25 mM ethylenediamine in pH 7.4 phosphate buffer prepared in 52% $H_2{}^{17}O$. The reaction was initiated by the addition of Co(II), and the spectrum was initiated 2 min after mixing. Instrumental conditions were the same as in Figure 5. The computer-simulated spectrum is shown by the dotted line, and the parameters are given in the text.

absorbance spectrum (data not shown) is indicative of O_2 binding by cobalt complexes with ethylenediamine and related ligands (*21*).

Neither free superoxide nor free hydrogen peroxide had any role in the formation of DMPO/•OH because the prior addition of SOD and catalase separately (data not shown) or together (Figure 6G) had no effect on the formation of the DMPO/•OH adduct. In addition, both ethanol and DMSO failed to inhibit DMPO/•OH radical adduct formation. When the reaction was carried out in a solution containing 52% $H_2{}^{17}O$ ($I = {}^5/_2$ for ^{17}O), additional hyperfine splitting from DMPO/•^{17}OH was observed, where $a^N = 14.9$ G, $a_\beta^H = 14.9$ G, and $a_\beta^O(^{17}O) = 4.6$ G (Figure 8). Computer simulation of the total signal from both the •^{16}OH and •^{17}OH adducts of DMPO yielded a (DMPO/•^{16}OH):(DMPO/•^{17}OH) ratio of 49:51, very close to the expected 48:52 ratio. Therefore, the DMPO/•OH adduct observed was formed from a reaction between DMPO and water and catalyzed by the cobalt complex. In contrast, no ^{17}O nuclear hyperfine splitting was observed in the spectrum of DMPO/•OOH formed from the reaction be-

tween unchelated Co(II) and H_2O_2 in phosphate solution containing 52% $H_2{}^{17}O$.

Discussion

Co(II) generates the superoxide radical from hydrogen peroxide in pH 7.4 phosphate buffer. From ^{17}O-labeling experiments, neither reduction of molecular oxygen (*16*) nor oxidation of water contributed to the formation of the superoxide radical trapped by DMPO. Thus, it is apparent from our results here and previous work (*16*) that noncomplexed Co(II) produces superoxide from hydrogen peroxide and that free hydroxyl radical is unlikely to be the oxidant responsible for degrading deoxyribose and hydroxylating aromatic compounds (*13*).

Chelation by NTA increases the amount of DMPO/•OOH detected by at least an order of magnitude. How the rapid oxidation of H_2O_2 to the superoxide radical occurred remains unclear; however, it seems unlikely that it involved the reduction of Co(II) to Co(I). Co(I) complexes are powerful reductants and are generally difficult to attain in aqueous solution (*20*). Furthermore, if a Co(I)–NTA transient species had formed in solution, it would have been expected to reduce H_2O_2 to •OH, but a simultaneous generation of DMPO/•OOH and DMPO/•OH was not observed. A more plausible explanation would be the dismutation of H_2O_2 in the presence of the Co(II) ion or Co(II)–NTA complex, where superoxide was liberated and the corresponding reduced product of hydrogen peroxide, formally either the •OH radical or hydroxide ion, remained tightly associated with the cobalt center.

In addition to the rapid appearance of the DMPO/•OOH EPR signal, the relatively slow formation of the DMPO/•OH adduct occurs during the reaction of the Co(II)–NTA complex with H_2O_2, presumably due to the oxidation of Co(II) to Co(III). The release of free hydroxyl radical in solution by this system apparently did not occur since it was not readily scavenged by DMSO and, hence, seems either to have remained tightly associated with the cobalt complex or to have been scavenged by the NTA ligand in a site-specific manner. Initially, such an active oxygen species was referred to as a "crypto-OH" radical (*22, 23*). On the other hand, the ease of the reaction of ethanol relative to DMSO with this species may reflect the ability of ethanol to penetrate to the sphere of hydration about the Co–NTA complex and more closely approach the metal center. This then implies that DMPO must also approach the metal center in order to form the DMPO/•OH adduct.

The formation of metal-bound •OH radicals may lead to site-specific reactions. Site-specific hydroxyl radical generation adequately accounts for the reaction between the Co(II)–deferoxamine complex and hydrogen peroxide. In this case, Co(II) was rapidly oxidized to Co(III) by H_2O_2 to generate the •OH radical in a Fenton-like manner. The hydroxyl radical formed may or may not exist as a free radical (i.e., it may exist as a metal-bound species), but it immediately reacted with the deferoxamine ligand at the cobalt center to form the well-characterized deferoxamine nitroxide radical (*18, 19*). Ethanol (up to a 400-fold excess over cobalt) was unable to scavenge the hydroxyl radical generated by this complex, further supporting the site-specific mechanism. Site-specific mechanisms have also been proposed for Co(II)-induced DNA damage (*5*) and deoxyribose degradation (*13, 15*) in the presence of H_2O_2. Our results clearly indicate that complexes between Co(II) and DNA or Co(II) and deoxyribose must occur first for the site-specific reactions to proceed. In the latter case, oxidative degradation of deoxyribose by Co(II) may not actually occur until other reagents necessary for the chemical analysis of the degradation products are added (*24*). The results with deferoxamine suggest that this ligand may have a positive protective effect against oxidative damage from Co(II) in cobalt intoxication.

It has been reported that Co(II) and H_2O_2 in the presence of ADP generate hydroxyl radicals (*5*). The results reported here show no evidence for such an assignment. ADP and citrate both inhibited formation of the superoxide radical from Co(II) and H_2O_2. More importantly, they did not promote the oxidation of Co(II) to Co(III) by H_2O_2 at any significant rate as shown in Figure 3C. ADP and H_2O_2 together, with or without Co(II), produced significant amounts of hydroxyl radical within 3 min after mixing (Figure 5F), even after the ADP solution was first incubated with Chelex resin in an attempt to remove trace metals. It seems unlikely, then, that the Co(II)–ADP system is a reliable model for studying the mechanism leading to DNA damage by Co(II) and H_2O_2 (*5*) and may actually moderate the toxicity of excess Co(II) in vivo.

The uptake of dioxygen by Co(II) complexes in solution with amino and polyamino ligands has been studied in some detail (*20, 25–29*) and is shown to occur also in our system when Co(II) was mixed with ethylenediamine (Figure 7). These complexes form dimers in aqueous solution, with the dioxygen molecule binding both cobalt atoms to give a Co–O–O–Co bridged structure (*30, 31*). Some complexes have a second bridging ligand, such as an amino or hydroxo group, to form a five-membered ring core structure within the cobalt dimer (*28*). Although the cobalt atoms in the amino dimer complex are formally considered to be in the Co(III) oxidation state with a μ-peroxo bridge (*30*), EPR data suggest that paramagnetic delocalization over all four Co–O–O–Co atoms occurs (*32*). Upon a one-electron oxidation, the bound dioxygen molecule is best considered as a superoxide bridge according to its O–O bond length (*31*).

DMPO was oxidized to the DMPO/•OH adduct by Co(II) and ethylenediamine in pH 7.4 phosphate buffer when O_2 was present. The mechanism for this reaction apparently did not involve attack on the DMPO by free •OH radicals. In fact, the generation of O-centered free radicals from O_2 was not significant in this system, since neither SOD nor hydroxyl radical scavengers (ethanol or DMSO) had any effect. Catalase also had no effect on the EPR signal of the DMPO/•OH adduct, indicating that free H_2O_2 was not necessary for this reaction. These results, then, strongly suggest a direct interaction between DMPO and the cobalt–ethylenediamine complex in solution.

The experiments with ^{17}O-enriched water demonstrate clearly that the hydroxyl adduct of DMPO formed in this system was a result of the reaction between DMPO and water. The reaction between a DMPO cation (formed from exposure of DMPO to ionizing radiation) and water has been reported (*33*). Oxidation of DMPO to its radical cation by a cobalt complex with ethylenediamine and O_2 also may occur. This highly unstable radical cation would then react with water to form the DMPO/•OH adduct. Alternatively, a mechanism where nucleophilic attack by water at the unsaturated carbon of the DMPO ring occurs may have been induced through a direct interaction between DMPO and the cobalt complex. Such a mechanism has recently been proposed for DMPO and aqueous Fe(III) (*34*) and seems more plausible for the cobalt system described here than the generation of the DMPO radical cation.

In summary, the generation of active oxygen species from Co(II) is highly dependent on the ligation about the

cobalt. With NTA, Co(II) is responsible for the rapid production of superoxide from H_2O_2, as well as the slower production of a strong oxidant associated with the oxidation of Co(II) to Co(III) by H_2O_2. In contrast, oxidation of Co(II) by H_2O_2 is rapid when chelated by deferoxamine, where the deferoxamine ligand is itself oxidized to its nitroxide radical, but no superoxide radical is detected. On the other hand, no free radicals are detected from Co(II) and H_2O_2 in the presence of either ADP, citrate, or EDTA, even though Co(II) is oxidized by H_2O_2 in the EDTA complex. When chelated by ethylenediamine, Co(II) causes DMPO to be oxidized to its DMPO/$^{\bullet}$OH adduct without formation of free hydroxyl radical. This latter result should be regarded as a caveat when using spin traps in the presence of transition metals or, perhaps, certain redox-active metalloenzymes.

Studies on the mechanism of Co(II)-induced oxidative damage to biomolecules should be interpreted cautiously if the ligation about the cobalt center and the resulting chemistry has not been adequately determined, especially if a free-radical mechanism is invoked. Unlike Fe(II), Co(II) does not readily generate free hydroxyl radicals in the presence of H_2O_2 in vitro. The presence of strongly bound N ligands facilitates the oxidation of Co(II) to Co(III), but oxidizing O-centered radicals are not necessarily generated or, if generated, cause highly site-specific oxidative damage to the cobalt ligands. A very recent study has linked Co(II) toxicity in the lungs of Syrian gold hamsters to a mechanism involving oxidative stress (*35*). While oxidative stress from Co(II) complexes formed with biomolecules in vitro or in vivo may occur (*5*, *11*, *12*, *35*), it seems unlikely that it is a result of free hydroxyl radical generation.

Registry No. Superoxide, 11062-77-4; $^{\bullet}$OH, 3352-57-6; Co, 7440-48-4; H_2O_2, 7722-84-1; O_2, 7782-44-7.

References

(1) Kazantzis, G. (1981) Role of cobalt, iron, lead, manganese, mercury, platinum, selenium, and titanium in carcinogenesis. *Environ. Health Perspect.* **40**, 143–161.

(2) Heath, J. C. (1954) Cobalt as a carcinogen. *Nature (London)* **173**, 822–823.

(3) Shabaan, A. A., Marks, V., Lancaster, M. C., and Dufeu, G. N. (1977) Fibrosarcomas induced by cobalt chloride ($CoCl_2$) in rats. *Lab. Anim.* **11**, 43–46.

(4) Kawanishi, S., Inoue, S., and Yamamoto, K. (1989) Hydroxyl radical and singlet oxygen production and DNA damage induced by carcinogenic metal compounds and hydrogen peroxide. *Biol. Trace Elem. Res.* **21**, 367–372.

(5) Yamamoto, K., Inoue, S., Yamazaki, A., Yoshinaga, T., and Kawanishi, S. (1989) Site-specific DNA damage induced by cobalt(II) ion and hydrogen peroxide: role of singlet oxygen. *Chem. Res. Toxicol.* **2**, 234–239.

(6) Yamamoto, K., and Kawanishi, S. (1991) Site-specific DNA damage induced by hydrazine in the presence of manganese and copper ions. *J. Biol. Chem.* **266**, 1509–1515.

(7) Tephly, T. R., and Hibbein, P. (1971) The effect of cobalt chloride administration on the synthesis of hepatic microsomal cytochrome P-450. *Biochem. Biophys. Res. Commun.* **42**, 589–595.

(8) Maines, M. D., and Kappas, A. (1977) Regulation of cytochrome P-450-dependent microsomal drug-metabolizing enzymes by nickel, cobalt, and iron. *Clin. Pharmacol. Ther.* **22**, 780–790.

(9) Sasame, H. A., and Boyd, M. R. (1978) Paradoxical effects of cobaltous chloride and salts of other divalent metals on tissue levels of reduced glutathione and microsomal mixed-function oxidase components. *J. Pharmacol. Exp. Ther.* **205**, 718–724.

(10) Kadiiska, M., and Stoytchev, T. (1980) Effect of acute intoxication with some heavy metals on drug metabolism. *Arch. Toxicol. Suppl.* **4**, 363–365.

(11) Smith, A. G., and Smith, A. N. (1984) Effect of cobaltous chloride on aggregation of platelets from normal and afibrinogenaemic human blood. *Toxicol. Lett.* **23**, 349–352.

(12) Calabrese, E. J., Canada, A. T., and Sacco, C. (1985) Trace elements and public health. *Annu. Rev. Public Health* **6**, 131–146.

(13) Moorhouse, C. P., Halliwell, B., Grootveld, M., and Gutteridge, J. M. C. (1985) Cobalt(II) ion as a promotor of hydroxyl radical and possible 'crypto-hydroxyl' radical formation under physiological conditions. Differential effects of hydroxyl radical scavengers. *Biochim. Biophys. Acta* **843**, 261–268.

(14) Wills, E. D. (1965) Mechanisms of lipid peroxide formation: role of metals and haematin proteins in the catalysis of the oxidation of unsaturated fatty acids. *Biochim. Biophys. Acta* **98**, 238–251.

(15) Gutteridge, J. M. C. (1983) Antioxidant properties of caeruloplasmin towards iron- and copper-dependent oxygen radical formation. *FEBS Lett.* **157**, 37–40.

(16) Kadiiska, M. B., Maples, K. R., and Mason, R. P. (1989) A comparison of cobalt(II) and iron(II) hydroxyl and superoxide free radical formation. *Arch. Biochem. Biophys.* **275**, 98–111.

(17) Thacker, M. A., and Higginson, W. C. E. (1975) Kinetics of hydrolysis of di-μ-hydroxobis[nitrilotriacetatocobaltate(III)] to diaqua(nitrilotriacetato)cobalt(III), and some reactions of the latter with non-metallic substrates in aqueous solution. *J. Chem. Soc., Dalton Trans.* **1975**, 704–711.

(18) Morehouse, K. M., Flitter, W. D., and Mason, R. P. (1987) The enzymatic oxidation of Desferal to a nitroxide free radical. *FEBS Lett.* **222**, 246–250.

(19) Davies, M. J., Donkor, R., Dunster, C. A., Gee, C. A., Jonas, S., and Willson, R. L. (1987) Desferrioxamine (Desferal) and superoxide free radicals. *Biochem. J.* **246**, 725–729.

(20) Cotton, F. A., and Wilkinson, G. (1980) *Advanced Inorganic Chemistry: A Comprehensive Text*, 4th ed., pp 766–783, Wiley-Interscience, New York.

(21) Bijl, P., and De Vries, G. (1972) Uptake of oxygen by aqueous solutions containing cobalt(II) ions and ethylenediamine. *J. Chem. Soc., Dalton Trans.* **1972**, 303–304.

(22) Youngman, R. J., and Elstner, E. F. (1981) Oxygen species in paraquat toxicity: the crypto-OH radical. *FEBS Lett.* **129**, 265–268.

(23) Youngman, R. J. (1984) Oxygen activation: is the hydroxyl radical always biologically relevant? *Trends Biochem. Sci.* **9**, 280–283.

(24) Halliwell, B., and Gutteridge, J. M. C. (1981) Formation of a thiobarbituric-acid-reactive substance from deoxyribose in the presence of iron salts. *FEBS Lett.* **128**, 347–352.

(25) McLendon, G., and Martell, A. E. (1976) Inorganic oxygen carriers as models for biological systems. *Coord. Chem. Rev.* **19**, 1–39.

(26) Henrici-Olivé, G., and Olivé, S. (1974) Activation of molecular oxygen. *Angew. Chem., Int. Ed. Engl.* **13**, 29–38.

(27) Harris, W. R., Murase, I., Timmons, J. H., and Martell, A. E. (1978) Chelating tendencies of pyridyl-containing polyamines and oxygenation of the cobaltous complexes. *Inorg. Chem.* **17**, 889–894.

(28) Barraclough, C. G., Lawrance, G. A., and Lay, P. A. (1978) Characterization of binuclear μ-peroxo and μ-superoxo cobalt(III) amine complexes from Raman spectroscopy. *Inorg. Chem.* **17**, 3317–3322.

(29) Ochiai, E.-I. (1973) Oxygenation of cobalt(II) complexes. *J. Inorg. Nucl. Chem.* **35**, 3375–3389.

(30) Vannerberg, N.-G. (1965) The crystal structure of decammine-μ-peroxodicobalt tetrathiocyanate. *Acta Crystallogr.* **18**, 449–453.

(31) Vannerberg, N.-G., and Brosset, C. (1963) The crystal structure of decammine-μ-peroxodicobalt pentanitrate. *Acta Crystallogr.* **16**, 247–251.

(32) Ebsworth, E. A. V., and Weil, J. A. (1959) Paramagnetic resonance absorption in peroxo–dicobalt complexes. *J. Phys. Chem.* **63**, 1890–1900.

(33) Chandra, H., and Symons, M. C. R. (1986) Hydration of spin-trap cations as a source of hydroxyl adducts. *J. Chem. Soc., Chem. Commun.* **1986**, 1301–1302.

(34) Makino, K., Hagiwara, T., Hagi, A., Nishi, M., and Murakami, A. (1990) Cautionary note for DMPO spin trapping in the presence of iron ion. *Biochem. Biophys. Res. Commun.* **172**, 1073–1080.

(35) Lewis, C. P. L., Demedts, M., and Nemery, B. (1991) Indices of oxidative stress in Hamster Lung following exposure to cobalt(II) ions: *in vivo* and *in vitro* studies. *Am. J. Respir. Cell Mol. Biol.* **5**, 163–169.